

Unusual Temperature Dependence of Band Dispersion in $\text{Ba}(\text{Fe}_{1-x}\text{Ru}_x)_2\text{As}_2$ and its Consequences for Antiferromagnetic Ordering

R. S. Dhaka,¹ S. E. Hahn,¹ E. Razzoli,² Rui Jiang,¹ M. Shi,² B. N. Harmon,¹ A. Thaler,¹ S. L. Bud'ko,¹ P. C. Canfield,¹ and Adam Kaminski^{1,*}

¹Ames Laboratory and Department of Physics and Astronomy, Iowa State University, Ames, Iowa 50011, USA

²Swiss Light Source, Paul Scherrer Institut, CH-5232 Villigen PSI, Switzerland

(Received 29 May 2012; published 6 February 2013)

We have performed detailed studies of the temperature evolution of the electronic structure in $\text{Ba}(\text{Fe}_{1-x}\text{Ru}_x)_2\text{As}_2$ using angle resolved photoemission spectroscopy. Surprisingly, we find that the binding energy of both hole and electron bands changes significantly with temperature in both pure and Ru substituted samples. The hole and electron pockets are well nested at low temperature in unsubstituted (BaFe_2As_2) samples, which likely drives the spin density wave and resulting antiferromagnetic order. Upon warming, this nesting is degraded as the hole pocket shrinks and the electron pocket expands. Our results demonstrate that the temperature dependent nesting may play an important role in driving the antiferromagnetic-paramagnetic phase transition.

DOI: [10.1103/PhysRevLett.110.067002](https://doi.org/10.1103/PhysRevLett.110.067002)

PACS numbers: 74.25.Jb, 74.62.Dh, 74.70.-b, 79.60.-i

The phase transition from antiferromagnetic (AFM) to paramagnetic (PM) order is believed to play a crucial role in the emergence of high temperature superconductivity in iron arsenic high temperature superconductors [1–5]. The associated transition temperature can be controlled by tuning parameters such as chemical substitution [6–19] or pressure [20–22]. The superconducting dome exists in the phase diagram surrounding the point where the AFM/PM phase transition temperature intersects $T = 0$ axis and it is believed that the AFM fluctuations are the glue pairing the electrons. Understanding the microscopic origin of this phase transition and the role of electronic structure is a prerequisite to validating the pairing mechanism and will likely aid the search for new superconducting materials. Our earlier studies [23] indicated that the AFM/PM phase transition is accompanied by a two- to three-dimensional change of the electronic structure. Fermi surface (FS) nesting is believed to play an important role in the emergence of the spin density wave (SDW) and AFM order [24,25]; however, a detailed understanding is still lacking. Data from the chemical substitution yield only a partially consistent picture here. It is now well established that substitutions of Fe with Co, Ni or Pd increase the carrier concentration and shift the chemical potential higher (see, for example, Refs. [9,26,27]). This of course would worsen the FS nesting conditions, and naturally lead to weakening of the SDW. A curious case is substitution of Fe with isoelectronic Ru, which results in a phase diagram similar to other substitutions (albeit for much higher Ru concentrations), but it was demonstrated to have negligible effects on the band dispersion up to 40% [28]. It appears that the SDW in this case is suppressed without significant change of the nesting condition and we speculated that magnetic dilution by less magnetic Ru may play a role in such a case [28].

In metallic materials, in absence of phase transitions, temperature has a negligible effect on the band structure, and is mostly limited to changes of the occupation close to the chemical potential (Fermi function) and changes of the quasiparticle lifetime reflected in the width of the spectral function measured by angle resolved photoemission spectroscopy (ARPES). It should be noted that band shifts are common in semiconductors [29] due to temperature induced changes in carrier concentration, mobility, and photoexcitation. Those do not play a role in metals since metals have a well defined chemical potential and significant DOS at E_f .

In this Letter, we demonstrate that the band structure of one of the prototypical iron arsenic materials is changing significantly with temperature; in both pure and Ru substituted BaFe_2As_2 samples we observe significant shifts in the energy position of the bands. Upon increasing temperature the hole band moves to higher binding energy and eventually sinks below E_f close to room temperature. The electron band also moves to higher binding energy with increasing temperature and the corresponding electron pocket becomes larger. While it is not clear at present if the Luttinger [30] sum rule is violated in these materials, this rather strange behavior destroys the nesting between electron and hole pockets present at low temperatures. Our finding explains the nearly linear decrease of the AFM transition temperature with increasing chemical substitution. It also points to a scenario where the AFM transition is driven by the weakening of nesting with temperature rather than thermal fluctuations alone.

Single crystals of $\text{Ba}(\text{Fe}_{1-x}\text{Ru}_x)_2\text{As}_2$ were grown out of self-flux using conventional high-temperature solution growth techniques [16,31]. The ARPES measurements were performed at ALS beam line 10.0.1 (linear horizontal polarization), the SLS Surface and Interface

Spectroscopy beam line (linear vertical polarization) and using a He II laboratory based system. The energy and angular resolution was set at 15 meV and 0.3° , respectively. *Ab initio* calculations were performed with VASP [32,33] using PAW pseudo-potentials [34,35] and utilizing the local density approximation (LDA) and Perdew-Burke-Ernzerhof (PBE) exchange-correlation functionals [36]. Experimental lattice parameters of $a = 3.9624$, $c = 13.0168$, and $z_{As} = 0.3545$ are used from Ref. [37].

Figures 1(a)–1(d) show the band dispersion maps for the parent compound BaFe_2As_2 measured at various temperatures using 35 eV ($k_z \approx 2\pi/c$) photon energy, i.e., the upper edge of the first Brillouin zone (Z point) [38]. The second set of measurements were performed using 63 eV photons, i.e., the center of the zone (Γ point) and the results are shown in Figs. 1(g)–1(k). All data were divided by resolution broadened Fermi functions to reveal band behavior in the proximity to the chemical potential. At low temperature, the hole band at the center of the BZ crosses the chemical potential at roughly $\pm 0.2\pi/a$ resulting in a holelike Fermi surface sheet (see also Fig. 2). With increasing temperature this band moves down, to larger binding energies, and at around 200 K, the top of the band moves very close to the chemical potential. Corresponding momentum distribution curves (MDC's), radii of the FS sheets, and MDC widths are plotted in panels on the right. Here the two well separated MDC peaks present at low temperature move closer together and merge into flat top peak signifying significant (factor of 2) reduction of the

size of the hole pocket. Those changes are accompanied by an increase in the MDC width, evident from raw data as well results of fitting in panels (f) and (m). Whereas the increase of the MDC width may be associated with the paramagnetic-antiferromagnetic-orthorhombic(tetragonal-orthorhombic) transition at $T \sim 134$ K, the downward movement of the band seems to occur even above that temperature. In order to visualize the changes of the hole FS sheet, we plot the ARPES intensity maps measured at the chemical potential in Fig. 2. The circular shape of this sheet, present at low temperature, shrinks and becomes a spot as the top of the band approaches the value of the chemical potential. It is clear from these data that the size of this FS sheet decreases with increasing temperature, which will affect nesting in a very profound way. The above changes are strongest close to the top and bottom edges of the BZ along the k_z direction. In Fig. 3, we plot the ARPES intensity along the (1,1,0) direction as a function k_z momentum. The large hole pocket present at the bottom and top edges of the zone ($k_z \sim 18\pi/c$) shrinks with temperature, whereas the dispersion close to center of the zone remains mostly unaffected.

In the pure BaFe_2As_2 samples, the band structure at low temperatures will of course be affected by the presence of the antiferromagnetic order. Since the electronic structure of Ru substituted samples, for $x \leq 0.40$ are almost identical [28], we can access low temperatures in the paramagnetic state by choosing finite x values with suppressed magnetic-structural phase transitions [16]. To verify that the temperature induced changes of the band structure are not caused

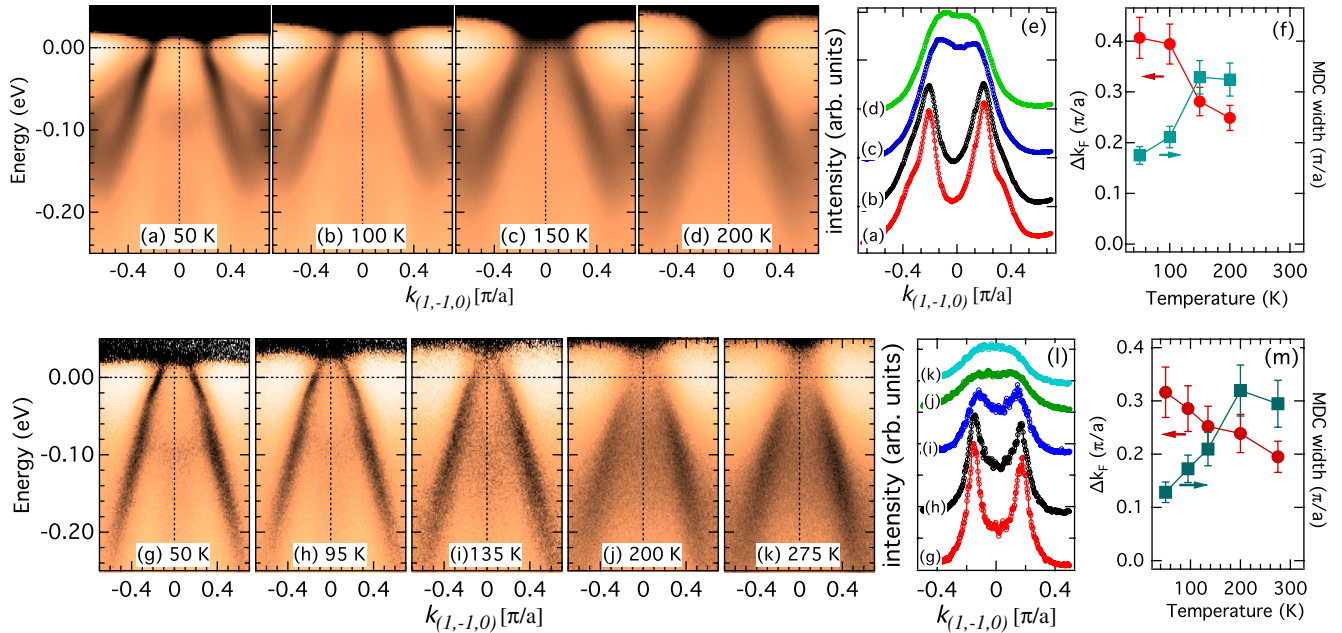


FIG. 1 (color online). The band dispersion data of the parent BaFe_2As_2 compound measured with (a)–(d) $h\nu = 35$ eV (linear horizontal polarization) and (g)–(k) $h\nu = 63$ eV (linear vertical polarization) for various sample temperature. (e), (l) The MDCs at E_F . (f), (m) The extracted Fermi surface calipers Δk_F and width of the MDC's plotted as a function of temperature.

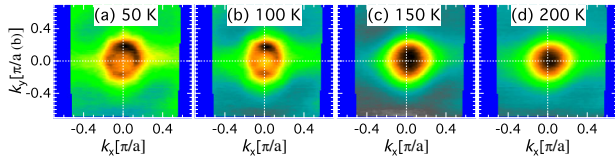


FIG. 2 (color online). (a)–(d) The FS maps of BaFe_2As_2 measured with $h\nu = 35$ eV (linear horizontal polarization) at various sample temperatures.

by an AFM phase transition, we performed similar measurements using $\text{Ba}(\text{Fe}_{1-x}\text{Ru}_x)\text{As}_2$ for $x = 0.28$ and 0.36 . The resulting ARPES intensities measured at several temperatures are shown for the hole band in Figs. 4(a)–4(d) and for the electron band in Figs. 4(e)–4(h); for $x = 0.36$ the AF transition is fully suppressed and all data are taken in the paramagnetic or tetragonal state. With increasing temperature, both the hole and electron bands move to a higher binding energy, similar to unsubstituted BaFe_2As_2 . As a result, the diameter of the hole pocket decreases and that of the electron pocket increases with increasing temperature. Therefore, nesting present at low temperatures between the hole and electron pockets weakens significantly upon warming up. To quantify this effect, we extracted the diameter of both pockets as a function of temperature by fitting the MDC's with Lorentzians. Results are plotted in Fig. 5. At 50 K the diameters of both the hole and electron pockets are close to $0.4\pi/a$, which corresponds to near nesting conditions. Upon warming up to 300 K, the diameter of the hole pocket decreases to $\sim 0.32\pi/a$, while the diameter of the electron pocket increases to $0.48\pi/a$, which obviously destroys the nesting. The apparent net increase of the Fermi surface volume does not necessarily imply violation of the Luttinger sum rule [30]. It is possible that two other Fermi sheets that are not visible in this geometry due to matrix elements (one electron in the corner of the BZ and one hole in the center of the BZ), change in opposite ways, thus preserving the carrier count. We cannot, however, exclude completely the possibility that the Luttinger sum rule is violated in

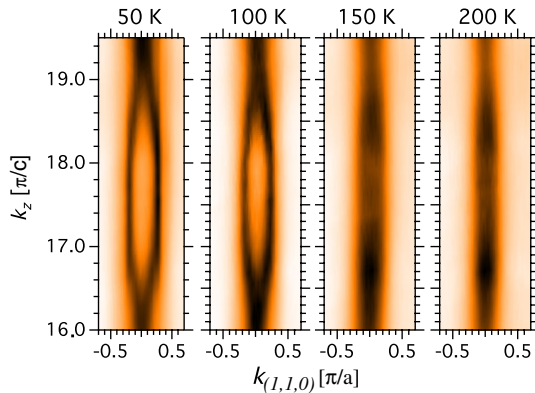


FIG. 3 (color online). The hole Fermi surface maps of BaFe_2As_2 (at various sample temperatures) along the $k_{||}-k_z$ plane measured around the center of the BZ by changing $h\nu$.

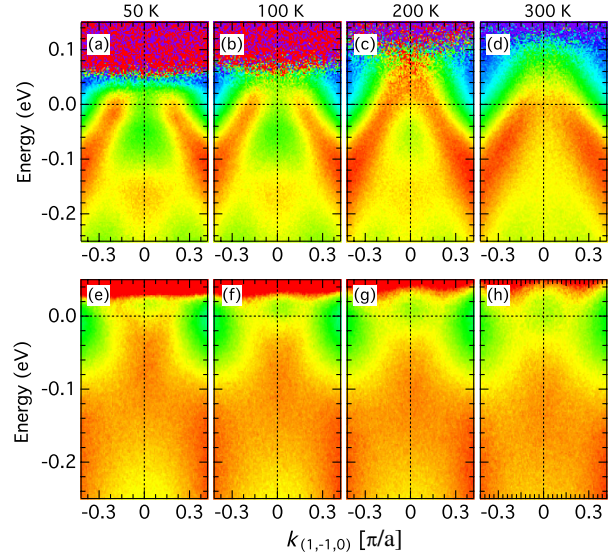


FIG. 4 (color online). The band dispersion plots for $\text{Ba}(\text{Fe}_{1-x}\text{Ru}_x)\text{As}_2$, $x = 0.36$ sample as a function of temperature. (a)–(d) hole pocket at the center of the BZ, (e)–(h) electron pocket at the planar corner of the BZ. Data measured with photon energy $h\nu = 40.8$ eV.

these materials due to, e.g., charge localization effects. We repeated the measurements, while cycling the sample temperature to ensure that this is an intrinsic effect and not due to aging of the sample surface. Similar data was also obtained for $x = 0.28$ (not shown) demonstrating that this effect does not change with Ru substitution. We should emphasize that, at these Ru substitution levels, the samples do not display AFM order at low temperatures despite presence of apparent nesting. We note that the AFM nesting vector has a component along the z direction. We can compare the size of both pockets at the same value of k_z because the electron pocket is quasi-2D and its diameter does not change significantly along the z direction [23].

Our findings explain the spectral behavior reported in optics measurements. Nesting in pnictides does not involve

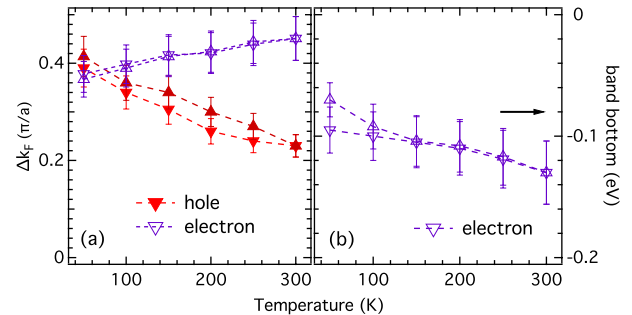


FIG. 5 (color online). Dependence of the size of the hole and electron pockets on temperature for $x = 0.36$ measured with $h\nu = 40.8$ eV. (a) Diameter (Δk_F) of hole and electron pockets as a function of temperature, (b) energy position of the bottom of electron pocket as a function of temperature.

TABLE I. Relaxed value of the internal arsenic position z_{As} for different values of the lattice parameter a . $\Delta a/a = 0.0\%$ and 0.6% correspond to 0 K and 300 K, respectively.

$\Delta a/a$	z_{As} (LDA)	z_{As} (PBE)	z_{As} (exp.)
0.0%	0.3413($\alpha = 30.96^\circ$)	0.3452($\alpha = 32.02^\circ$)	
0.6%	0.3402(30.65°)	0.3442(31.75°)	0.3545(34.47°)

whole sheets of the FS, but rather their small portions, where the overlaps between electron and hole pockets are connected by the ordering vector [26,38]. In such cases, the temperature induced shift of bands in energy significantly below T_N will only move the location of the portions of FS affected by SDW gap in the momentum space (the pattern of FS reconstruction will change) rather than significantly change the SDW gap. This is consistent with optics data [39], where both temperature dependent weight transfer and small changes in mid-infrared peak position are present well below T_N . As T_N is approached, the SDW gap will close in BCS-like fashion [24,25] due to the combination of thermal fluctuations and weakened nesting conditions, since portions of the FS that can be overlapped by the ordering vector vanish at high temperatures.

The large temperature induced changes of the band dispersion are indeed very unusual and unexpected. To the best of our knowledge, no such changes were reported in any of the studied systems before. The most obvious explanation of this effect is subtle changes in relative atomic positions due to thermal expansion. It is well known that the energy positions of the bands are very sensitive to the Fe-As distance. If the Fe-As distance changes significantly with the temperature, this may explain our observations. We have therefore performed band structure calculations using density functional theory for the parent compound BaFe_2As_2 in order to understand the changes of the diameter of the pockets (Δk_F) with temperature. Since we were not able to find temperature dependent crystallographic data detailing the changes in ionic position with temperature, we made extrapolations based on tetragonal structure, and thermal expansion data [40]. Room temperature parameters were used for a and c . Next, we reduced

a by the amount measured in the thermal expansion data. Initial calculations using the measured atomic positions show a band with $d_{x^2-y^2}$ character shifting downward by 17 and 15 meV for LDA and PBE exchange correlation functionals. This is approximately half the observed change (35 ± 5 meV) by fitting tops of the energy distribution curves peaks with a Gaussian in ARPES data. A band with d_{xz}/d_{yz} character shifts downward by about 5 meV. At the electron pocket, bands with d_{xz}/d_{yz} character shift downwards by about 5 meV.

Using room temperature parameters for a and c , we allowed z_{As} to relax such that all forces on the atoms equaled zero. We then reduced a by the amount measured in the thermal expansion data and again determined z_{As} associated with this value of a . Calculated and measured values of z_{As} are shown in Table I. Near the Z (Γ) point the band with $d_{x^2-y^2}$ character shifts downward by 28 and 25 meV with LDA and PBE exchange-correlation functionals, respectively. For the electron pocket the changes are small and almost no observable shift is present in the upper band (d_{xz} character), while, the lower band has d_{yz} character and shifts downwards by about 6 meV. We note that the calculated shifts are significantly smaller than experimental ones, most likely due to lack of precise temperature dependent crystallographic data and approximations used in the calculations. These numerical results demonstrate that while changes in atomic positions are likely contributing to the observed shift of the band energies, they do not fully account for large shifts observed in the experimental data. Calculated band dispersions for low and high temperatures are shown in Fig. 6.

In conclusion, we demonstrated that the band structure of pure and Ru substituted BaFe_2As_2 changes appreciably with temperature. The nesting conditions leading to the SDW and present at low temperature become weaker upon warming up. This likely contributes to destruction of AFM order at higher temperatures. In essence, increasing temperature has a similar effect on the band structure and nesting as Co substitution. This explains why the AFM/PM transition in the phase diagram is almost a straight line. At higher Co concentration, the nesting and AFM order is suppressed by smaller increase of the temperature.

We would like to thank Rafael Fernandez, Andy Millis, and Andrey Chubukov for very useful discussions, Sung-Kwan Mo at the ALS and staff at SLS for their excellent instrumental support. The work at the Ames Laboratory was supported by the Department of Energy, Basic Energy Sciences under Contract No. DE-AC02-07CH11358.

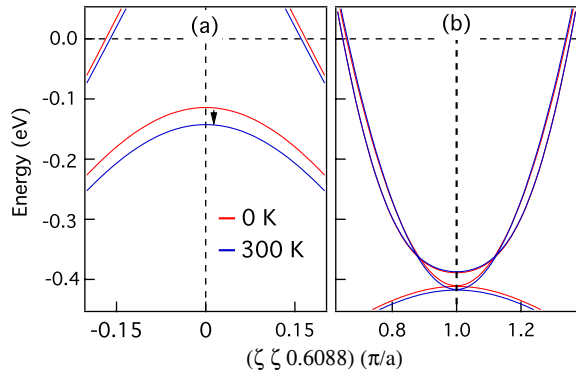


FIG. 6 (color online). Band structure calculation for BaFe_2As_2 (a) the Z hole pocket and (b) the X electron pocket.

- *kaminski@ameslab.gov
- [1] Y. Kamihara, T. Watanabe, M. Hirano, and H. Hosono, *J. Am. Chem. Soc.* **130**, 3296 (2008).
- [2] X.H. Chen, T. Wu, G. Wu, R.H. Liu, H. Chen, and D.F. Fang, *Nature (London)* **453**, 761 (2008).
- [3] T.Y. Chen, Z. Tesanovic, R.H. Liu, X.H. Chen, and C.L. Chien, *Nature (London)* **453**, 1224 (2008).
- [4] G.F. Chen, Z. Li, D. Wu, G. Li, W.Z. Hu, J. Dong, P. Zheng, J.L. Luo, and N.L. Wang, *Phys. Rev. Lett.* **100**, 247002 (2008).
- [5] H. Takahashi, K. Igawa, K. Arii, Y. Kamihara, M. Hirano, and H. Hosono, *Nature (London)* **453**, 376 (2008).
- [6] M. Rotter, M. Tegel, and D. Johrendt, *Phys. Rev. Lett.* **101**, 107006 (2008).
- [7] A. S. Sefat, R. Jin, M. A. McGuire, B. C. Sales, D. J. Singh, and D. Mandrus, *Phys. Rev. Lett.* **101**, 117004 (2008); A. S. Sefat, A. Huq, M. A. McGuire, R. Jin, B. C. Sales, D. Mandrus, L. M. D. Cranswick, P. W. Stephens, and K. H. Stone, *Phys. Rev. B* **78**, 104505 (2008).
- [8] K. Sasmal, B. Lv, B. Lorenz, A. M. Guloy, F. Chen, Y.-Y. Xue, and C.-W. Chu, *Phys. Rev. Lett.* **101**, 107007 (2008).
- [9] P. C. Canfield and S. L. Bud'ko, *Annu. Rev. Condens. Matter Phys.* **1**, 27 (2010).
- [10] D. C. Johnston, *Adv. Phys.* **59**, 803 (2010).
- [11] S. Jiang, H. Xing, G. Xuan, C. Wang, Z. Ren, C. Feng, J. Dai, Z. Xu, and G. Cao, *J. Phys. Condens. Matter* **21**, 382203 (2009); L. E. Klintberg, S. K. Goh, S. Kasahara, Y. Nakai, K. Ishida, M. Sutherland, T. Shibauchi, Y. Matsuda, and T. Terashima, *J. Phys. Soc. Jpn.* **79**, 123706 (2010).
- [12] Y.-Z. Zhang, H. C. Kandpal, I. Opahle, H. O. Jeschke, and R. Valenti, *Phys. Rev. B* **80**, 094530 (2009).
- [13] S. Sharma, A. Bharathi, S. Chandra, V. R. Reddy, S. Paulraj, A. T. Satya, V. S. Sastry, A. Gupta, and C. S. Sundar, *Phys. Rev. B* **81**, 174512 (2010); W. Schnelle, A. Leithe-Jasper, R. Gumeniuk, U. Burkhardt, D. Kasinathan, and H. Rosner, *Phys. Rev. B* **79**, 214516 (2009).
- [14] M. Tropeano *et al.*, *Phys. Rev. B* **81**, 184504 (2010).
- [15] H. Hodovanets, E. D. Mun, A. Thaler, S. L. Budko, and P. C. Canfield, *Phys. Rev. B* **83**, 094508 (2011).
- [16] A. Thaler, N. Ni, A. Kracher, J. Yan, S. Bud'ko, and P. Canfield, *Phys. Rev. B* **82**, 014534 (2010).
- [17] F. Rullier-Albenque, D. Colson, A. Forget, P. Thuery, and S. Poissonnet, *Phys. Rev. B* **81**, 224503 (2010).
- [18] S. Thirupathiah *et al.*, *Phys. Rev. B* **84**, 014531 (2011).
- [19] Z. R. Ye, Y. Zhang, F. Chen, M. Xu, Q. Q. Ge, J. Jiang, B. P. Xie, and D. L. Feng, *Phys. Rev. B* **86**, 035136 (2012).
- [20] M. S. Torikachvili, S. L. Bud'ko, N. Ni, and P. C. Canfield, *Phys. Rev. Lett.* **101**, 057006 (2008).
- [21] S. A. J. Kimber *et al.*, *Nat. Mater.* **8**, 471 (2009).
- [22] E. Colombier, S. L. Budko, N. Ni, and P. C. Canfield, *Phys. Rev. B* **79**, 224518 (2009).
- [23] C. Liu *et al.*, *Phys. Rev. Lett.* **102**, 167004 (2009).
- [24] W. Z. Hu, J. Dong, G. Li, Z. Li, P. Zheng, G. F. Chen, J. L. Luo, and N. L. Wang, *Phys. Rev. Lett.* **101**, 257005 (2008).
- [25] A. Lucarelli, A. Dusza, F. Pfuner, P. Lerch, J. G. Analytis, J.-H. Chu, I. R. Fisher, and L. Degiorgi, *New J. Phys.* **12**, 073036 (2010).
- [26] C. Liu *et al.*, *Nat. Phys.* **6**, 419 (2010).
- [27] C. Liu *et al.*, *Phys. Rev. B* **84**, 020509(R) (2011).
- [28] R. S. Dhaka *et al.*, *Phys. Rev. Lett.* **107**, 267002 (2011).
- [29] Y. Wakisaka *et al.*, *J. Supercond. Novel Magnetism* **25**, 1231 (2012).
- [30] J. M. Luttinger and J. C. Ward, *Phys. Rev.* **118**, 1417 (1960); J. M. Luttinger, *Phys. Rev.* **119**, 1153 (1960).
- [31] N. Ni, M. E. Tillman, J.-Q. Yan, A. Kracher, S. T. Hannahs, S. L. Bud'ko, and P. C. Canfield, *Phys. Rev. B* **78**, 214515 (2008).
- [32] G. Kresse and J. Hafner, *Phys. Rev. B* **47**, 558 (1993); **49**, 14251 (1994).
- [33] G. Kresse and J. Furthmüller, *Phys. Rev. B* **54**, 11169 (1996); *Comput. Mater. Sci.* **6**, 15 (1996).
- [34] P. E. Blöchl, *Phys. Rev. B* **50**, 17953 (1994).
- [35] G. Kresse and D. Joubert, *Phys. Rev. B* **59**, 1758 (1999).
- [36] J. P. Perdew and A. Zunger, *Phys. Rev. B* **23**, 5048 (1981); J. P. Perdew, K. Burke, and M. Ernzerhof, *Phys. Rev. Lett.* **77**, 3865 (1996); **78**, 1396 (1997).
- [37] M. Rotter, M. Tegel, and D. Johrendt, *Phys. Rev. B* **78**, 020503 (2008).
- [38] T. Kondo *et al.*, *Phys. Rev. B* **81**, 060507(R) (2010).
- [39] M. Nakajima *et al.*, *Proc. Natl. Acad. Sci. U.S.A.* **108**, 12238 (2011).
- [40] S. L. Bud'ko, N. Ni, S. Nandi, G. M. Schmiedeshoff, and P. C. Canfield, *Phys. Rev. B* **79**, 054525 (2009).